

# Magnetic Interactions in the Copper Complex (L-Aspartato)(1,10-phenanthroline)copper(II) Hydrate. An Exchange-Coupled Extended System with Two Dissimilar Copper Ions

Carlos D. Brondino<sup>†</sup> and Rafael Calvo<sup>\*,†,‡</sup>

Departamento de Física, Facultad de Bioquímica y Ciencias Biológicas, Universidad Nacional del Litoral, C.C. 530, 3000 Santa Fe, Argentina, and INTEC (CONICET-UNL), Güemes 3450, 3000 Santa Fe, Argentina

Ana María Atria and Evgenia Spodine

Facultad de Ciencias Químicas y Farmacéuticas, Universidad de Chile, Casilla 233, Santiago, Chile

Otaci-ro R. Nascimento

Instituto de Física de São Carlos, Universidade de São Paulo, C.P. 369, 13560 São Carlos, São Paulo, Brazil

Octavio Peña

Laboratoire de Chimie du Solide et Inorganique Moleculaire, URA 1495, Université de Rennes I, 35042 Rennes Cedex, France

Received August 28, 1996<sup>⊗</sup>

We report EPR measurements in single-crystal samples at the microwave frequencies 9.8 and 34.3 GHz and magnetic susceptibility measurements in polycrystalline samples for the ternary complex of copper with aspartic acid and phenanthroline, (L-aspartato)(1,10-phenanthroline)copper(II) hydrate. The crystal lattice of this compound is composed of two dissimilar copper ions identified as Cu(A) and Cu(B), which are in two types of copper chains called A and B, respectively, running parallel to the *b* crystal axis. The copper ions in the A chains are connected by the aspartic acid molecule, and those in the B chains by a chemical path that involves a carboxylate bridge and a hydrogen bond. Both chains are held together by a complex network of hydrogen bonds and by hydrophobic interactions between aromatic amines. Magnetic susceptibility data indicate a Curie–Weiss behavior in the studied temperature range (2–300 K). The EPR spectra at 9.8 GHz display a single exchange collapsed resonance for any magnetic field orientation, in the so-called strong exchange regime. Those at 34.3 GHz are within the so-called weak exchange regime and display two resonances which belong to each type of copper ion chain. The decoupling of the spectra at 34.3 GHz using a theory based on Anderson's model for the case of two weakly exchange coupled spins  $S = 1/2$  allows one to obtain the angular variation of the squares of the *g*-factor and the peak-to-peak line width of each resonance. This model also allows one to evaluate the exchange parameter  $|J_{AB}/k| = 2.7(6)$  mK associated with the chemical path connecting dissimilar copper ions. The line width data obtained for each component of the spectra at 34.3 GHz are analyzed in terms of a model based on Kubo and Tomita's theory, to obtain the exchange parameters  $|J_A/k| = 0.77(2)$  K and  $|J_B/k| = 1.44(2)$  K associated with the chemical paths connecting the similar copper ions of types A and B, respectively.

## Introduction

We are interested in the magnetic interactions in copper(II)–amino acid complexes [Cu(aa)]. In some of them the copper ions are arranged in infinite extended lattices having one or two magnetic dimensions. This originates interesting magnetic behavior, observed in magnetic susceptibility,<sup>1,2</sup> electron paramagnetic resonance (EPR),<sup>2,3</sup> and specific heat data.<sup>4,5</sup> Also,

in these compounds the copper ions are linked by different types of chemical paths, allowing evaluation of superexchange interactions transmitted over long distances via extended molecular bridges.

As part of our investigation we have studied the copper complexes of aspartic [Cu(asp)] and glutamic [Cu(glu)] acids and the ternary copper complexes of these amino acids with the aromatic amines (ar) phenanthroline (phen), bipyridine (bpy), and imidazole (im) [Cu(aa)ar].<sup>6</sup> The interesting property of these compounds is that asp and glu ions may coordinate to the metal ions in the usual bidentate way through the amino acid group, and through the carboxylate group of the amino acid side chain, but they can also bridge different metal centers, giving rise to polymetallic species. Thus, in the compounds

<sup>†</sup> Universidad Nacional del Litoral.

<sup>‡</sup> INTEC (CONICET-UNL).

<sup>⊗</sup> Abstract published in *Advance ACS Abstracts*, June 15, 1997.

(1) Newman, P. R.; Imes, J. L.; Cowen, J. A. *Phys. Rev. B* **1976**, *13*, 4093.

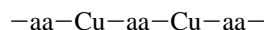
(2) Calvo, R.; Passeggi, M. C. G.; Novak, M. A.; Symko, O. G.; Oseroff, S. B.; Nascimento, O. R.; Terrile, M. C. *Phys. Rev. B* **1991**, *43*, 1074.

(3) Gennaro, A. M.; Levstein, P. R.; Steren, C. A.; Calvo, R. *Chem. Phys.* **1987**, *111*, 431.

(4) Siqueira, M. L.; Rapp, R. E.; Calvo, R. *Phys. Rev. B* **1993**, *48*, 3257.

(5) Rapp, R. E.; Souza, E. P. de; Godfrin, H.; Calvo, R. *J. Phys.: Condens. Matter* **1995**, *7*, 9595.

Cu(asp) and Cu(glu) the copper ions are in polymeric chains of the type



where the amino acid molecules bridge pairs of neighboring copper ions,<sup>7,8</sup> and the main goal of our previous studies<sup>8,9</sup> was the evaluation of the ability of the saturated  $\sigma$ -skeleton of the amino acid molecule as a superexchange interaction path between copper ions. The polymeric structure observed in Cu(asp) and Cu(glu) is modified in the ternary copper complexes Cu(aa)ar.<sup>6</sup> There, the aromatic amines compete with the functional group of the amino acid for the metal site, changing its molecular configuration. Thus, in some cases the coordination of the copper ions through the carboxylate group of the amino acid side chain is unfavorable, giving rise to compounds of the monomeric type. Another characteristic of the Cu(aa)ar complexes is the ability of the aromatic amines to give rise to intra- and intermolecular hydrophobic and stacking interactions. Such interactions are very important in nature, and they are responsible for the existence of distinct structures in biological compounds.<sup>10</sup> In Cu(aa)ar, the hydrophobic interactions, not only stabilize the ternary complexes but also are suggested to serve as chemical paths for superexchange interactions.<sup>11,12</sup>

Here we report a study of a ternary copper complex with L-aspartic acid and phenanthroline using electron paramagnetic resonance (EPR) and magnetic susceptibility measurements. Its crystal structure, recently reported elsewhere,<sup>13</sup> has two dissimilar copper(II) ions connected by various types of superexchange paths. The single-crystal EPR studies performed at 9.8 and 34.3 GHz reveal interesting physical properties. The spectra obtained at 9.8 GHz display a single exchange collapsed resonance, in the so-called strong exchange regime. Those at 34.3 GHz are within the so-called weak exchange regime and display two resonances. We treat the problem of the two-component EPR spectra using a theory based on Anderson's model for the case of two weakly exchange coupled spins  $S = 1/2$ <sup>14</sup> and analyze the results obtained in terms of the classical theories of exchange narrowing.<sup>14-18</sup> The experimental data analyzed in terms of these two models allow us to learn about the electronic properties of both types of copper ions and evaluate selectively the exchange parameters between specific spins in the crystal lattice.

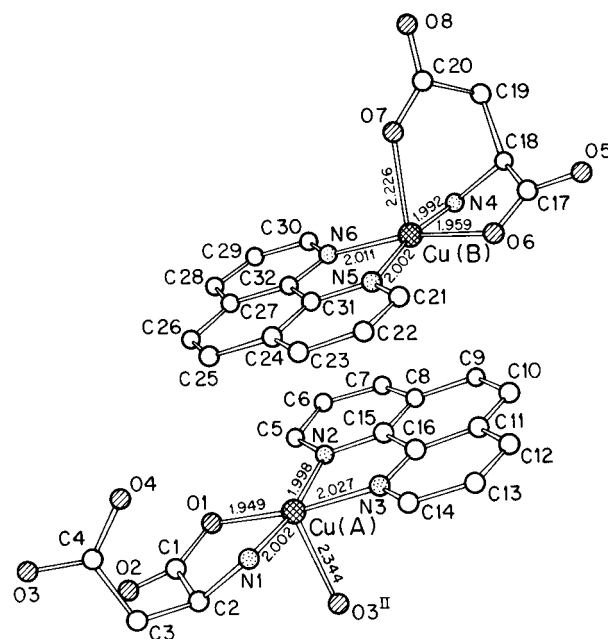


**Figure 1.** Coordination around the copper ions in Cu(asp)phen showing the interaction between two almost coplanar phenanthroline molecules belonging to dissimilar copper ions at the same symmetry position of the crystal lattice. The distances are given in angstroms.

### Description of the Crystal Structure

The structure of Cu(asp)phen<sup>13</sup> is monoclinic, space group  $P2_1$ ,  $z = 4$ , with lattice parameters  $a = 8.497(3)$ ,  $b = 9.902(3)$ ,  $c = 21.030(5)$  Å, and  $\beta = 92.14(1)^\circ$ . The crystal lattice is composed of two types of copper complexes, identified as Cu(A) and Cu(B) in Figure 1. The coordination geometries around the copper atoms in both complexes are approximately square pyramidal. The equatorial ligands of the Cu(A) and Cu(B) ions are the nitrogen atoms of the phenanthroline molecules and the nitrogen and oxygen atoms of the amino acid group of the asp molecules. As shown in Figure 1, in the Cu(A) complex the apical position is occupied by an oxygen atom (O3) of a neighboring aspartic acid molecule. In the Cu(B) complex this position is occupied by the oxygen O7, from the same aspartic acid molecule. Bonding distances in both complexes are similar, the only exception being the apical Cu(B)–O7 bond [2.226(5) Å], somewhat shorter than the corresponding Cu(A)–O3 bond [2.344(5) Å] (Figure 1).

Cu(A) as well as Cu(B) ions are in chains running parallel to the  $b$  crystal axis identified as A and B in Figure 2. Both chains are composed of two  $Cu^i(\alpha)$  ions ( $i = I$  and  $II$  and  $\alpha = A$  or  $B$ ) per unit cell, related by a rotation of  $180^\circ$  around the  $b$  axis, plus a translation. Copper ions in the general position  $x, y, z$  are labeled as  $Cu^I(\alpha)$ , while those at the symmetry-related position  $\bar{x}, 0.5 + y, \bar{z}$  are labeled as  $Cu^{II}(\alpha)$ . The copper ions in the A chains are bridged by asp molecules. Those in the B chains are bridged by two types of chemical paths, both involving a carboxylate bridge plus a hydrogen bond. One of them links neighboring Cu(B) ions from an equatorial position to an equatorial position [O6–C17–O5...H–N4], and the other from an apical position to an equatorial position [O7–C20–O8...H–N4] (Figure 2). Cu(A) and Cu(B) ions at the same symmetry position interact through the hydrophobic interaction between two almost coplanar aromatic amines which are separated by approximately 3.5 Å (Figure 1). Also, the A and B chains are held together by a complex network of hydrogen bonds that involve equatorial and apical copper ligands (Figure 2). They do not seem to make an important contribution to the

- (6) (a) Antolini, L.; Marcotriggiano, G.; Menabue, L.; Pellacani, G. C.; Saladini, M. *Inorg. Chem.* **1982**, *21*, 2263. (b) Antolini, L.; Marcotriggiano, G.; Menabue, L.; Pellacani, G. C. *Inorg. Chem.* **1983**, *22*, 141. (c) Antolini, L.; Marcotriggiano, G.; Menabue, L.; Pellacani, G. C.; Saladini, M.; Sola, M. *Inorg. Chem.* **1985**, *24*, 3621. (d) Antolini, L.; Battaglia, L. P.; Bonamartini Corradi, A.; Marcotriggiano, G.; Menabue, L.; Pellacani, G. C.; Saladini, M.; Sola, M. *Inorg. Chem.* **1986**, *25*, 2901.
- (7) Gramaccioli, C. M.; Marsh, R. E. *Acta Crystallogr.* **1966**, *21*, 594.
- (8) Calvo, R.; Steren, C. A.; Piro, O. E.; Rojo, T.; Zuñiga F. J.; Castellano, E. E. *Inorg. Chem.* **1993**, *32*, 6016.
- (9) Brondino, C. D.; Casado, N. M. C.; Passeggi, M. C. G.; Calvo, R. *Inorg. Chem.* **1993**, *32*, 2078.
- (10) Fisher, B. E.; Sigel, H. *J. Am. Chem. Soc.* **1980**, *102*, 2998.
- (11) Folgado, J. V.; Ibañez, R.; Coronado, E.; Beltrán, D.; Savariault, J. M.; Galy, J. *Inorg. Chem.* **1988**, *27*, 19.
- (12) Brondino, C. D.; Calvo, R.; Atria, A. M.; Spodine, E.; Peña, O. *Inorg. Chim. Acta* **1995**, *228*, 261.
- (13) Baggio, R. F.; Calvo, R.; Brondino, C. D.; Garland, M. T.; Atria, A. M.; Spodine, E. *Acta Crystallogr.* **1995**, *C51*, 382.
- (14) Anderson, P. W. *J. Phys. Soc. Jpn.* **1954**, *9*, 316.
- (15) Anderson, P. W.; Weiss, P. R. *Rev. Mod. Phys.* **1953**, *25*, 269.
- (16) Kubo, R.; Tomita, K. *J. Phys. Soc. Jpn.* **1954**, *9*, 888.
- (17) Bencini, A.; Gatteschi, D. *Electron Paramagnetic Resonance of Exchange Coupled Systems*; Springer: Berlin, 1989.
- (18) Abragam, A. *The Principles of Nuclear Magnetism*; Oxford University Press: London, 1961.

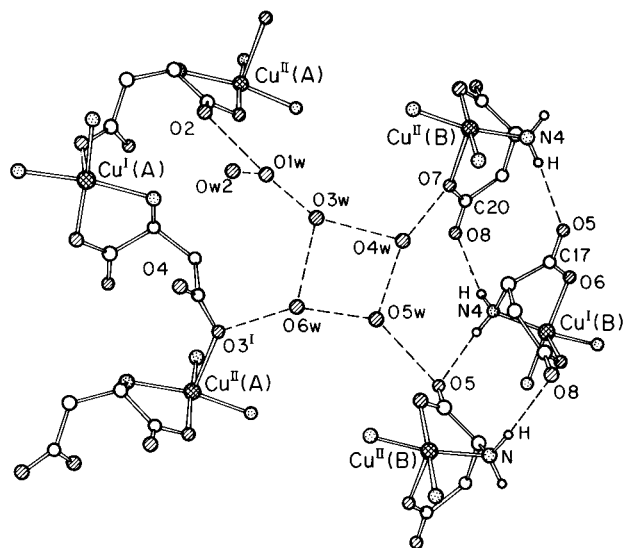


**Figure 2.** Copper ion chains in Cu(asp)phen. Both chains are held together by a complex network of hydrogen bonds involving the water molecules of solvation.

transmission of the superexchange interaction in this compound and therefore are not analyzed in detail.

### EPR Spectra of an Extended System in the Strong and Weak Exchange Limits

Within the linear response theory, the absorption spectrum observed in EPR experiments is given by

$$I(\omega) \propto \frac{\chi''}{\omega} = \frac{V}{2kT} \int_{-\infty}^{\infty} \langle \mathcal{M}_{h1}(t) \mathcal{M}_{h1} \rangle e^{-i\omega t} dt = \frac{V}{2kT} \langle \mathcal{M}_{h1} \mathcal{M}_{h1} \rangle \int_{-\infty}^{\infty} \varphi(t) e^{-i\omega t} dt \quad (1)$$

where  $\chi''$  is the dynamical susceptibility,  $\omega$  is the microwave frequency,  $k$  is the Boltzmann constant, and  $T$  is the temperature.  $\mathcal{M}_{h1}$  is the component of the magnetization operator along the direction of the microwave magnetic field  $\mathbf{B}_1$ , perpendicular to the applied static magnetic field  $\mathbf{B}$ , and  $\mathcal{M}_{h1}(t)$  is its time dependence.  $\varphi(t)$  is called the relaxation function, and  $\langle \dots \rangle$  indicates a thermal average calculated over the spin system. Equation 1 relates the absorption spectrum observed in EPR experiments to the Fourier transform of  $\varphi(t)$ .

Now we will briefly analyze the main characteristics of the absorption spectrum of an extended system with  $n$  magnetically nonequivalent copper sites per unit cell which, in the absence of exchange interactions between these copper sites, absorbs radiation at the frequencies  $\omega_1, \omega_2, \dots, \omega_n$ . In the strong exchange limit these  $n$  resonances collapse to a single line. In this case the absorption spectrum  $I(\omega)$  may be calculated using the exchange narrowing theories of Anderson<sup>14,15</sup> and Kubo and Tomita.<sup>16,17</sup> To perform this calculation it is convenient to write the Zeeman Hamiltonian of the system as<sup>9</sup>

$$H_Z = H_Z^0 + H_Z' \quad (2)$$

where

$$H_Z^0 = \mu_B \mathbf{S} \cdot \mathbf{g} \cdot \mathbf{B} \quad (2a)$$

$$\mathbf{S} = \sum_{i=1,n} \mathbf{S}_i \quad (2b)$$

is the total spin of the system,

$$\mathbf{g} = \frac{1}{n} \sum_{i=1,n} \mathbf{g}_i \quad (2c)$$

is the crystal  $\mathbf{g}$ -tensor defined as the average of the  $n$  molecular  $\mathbf{g}$ -tensors associated with each magnetically nonequivalent copper ion, and  $\mu_B$  is the Bohr magneton.  $H_Z^0$  in eq 2 is the main contribution to the Zeeman Hamiltonian.  $H_Z'$  is a smaller contribution, called residual Zeeman interaction, which arises when there are anisotropic magnetically nonequivalent spins in the crystal lattice. Taking into account eq 2, the total Hamiltonian of the system can be divided into a main contribution ( $H_0$ ) plus a perturbation ( $H'$ ),

$$H = H_0 + H' = H_Z^0 + H_{ex} + H' \quad (3)$$

where  $H_Z^0$  was defined in eq 2a, and

$$H_{ex} = -\frac{1}{2} \sum_{ij} J_{ij} \mathbf{S}_i \cdot \mathbf{S}_j$$

is the Heisenberg exchange interaction. The perturbation  $H'$  includes interactions such as residual Zeeman, hyperfine, dipole-dipole, and anisotropic and antisymmetric exchange. Thus, considering only the terms of  $H'$  that commute with  $H_Z^0$  for the evaluation of the relaxation function  $\varphi(t)$ , eq 1 predicts a resonance having a Lorentzian shape whose position is given by eq 2a. Each term of  $H'$  produces a broadening of the EPR line, given in field units by

$$\Delta B_i = (M_i^2 / g \mu_B \hbar) / \omega_{ex}^i \quad (4)$$

In eq 4  $M_i^2$  is the second moment of the contribution  $H'_i$  to  $H'$ , and  $\omega_{ex}^i$  is the corresponding exchange frequency produced by  $H_{ex}$  because  $H'_i$  and  $H_{ex}$  do not commute.<sup>14,16,17</sup> The perturbations included in eq 3 contribute to the line width with frequency independent angular functions, the only exception being the contribution of the Zeeman residual interaction.<sup>17,19</sup>

In the weak exchange limit, the exchange interaction is unable to collapse the  $n$  individual resonances. Anderson showed that in this regime and in the absence of saturation effects the relaxation function becomes<sup>14</sup>

$$\varphi(t) = \mathbf{W} \cdot \exp\{i(\omega + \boldsymbol{\pi})t\} \cdot \mathbf{1} \quad (5)$$

where the components of the vector  $\mathbf{W}$  are proportional to the occupation probabilities of the different states of the system,  $\mathbf{1}$  is a vector with all components equal to unity,  $\omega$  is a diagonal matrix whose elements are the absorption frequencies  $\omega_i$ , and  $\boldsymbol{\pi}$  is a matrix whose elements give the transition probabilities between the different spin states. As a generalization of Anderson's approach,<sup>14</sup> the Fourier transform in eq 1 can be solved<sup>20</sup> without explicit diagonalization of the matrix in eq 5, to obtain the line shape function  $I(\omega)$

$$I(\omega) \propto \text{Re } \mathbf{W} \cdot [i(\omega - \omega \mathbf{E}) + \boldsymbol{\pi}]^{-1} \cdot \mathbf{1} \quad (6)$$

where  $\omega \mathbf{E}$  is the unit matrix  $\mathbf{E}$  times the constant  $\omega$ .

Anderson solved the case of two spins  $S = 1/2$  with equal absorption probability ( $W_1 = W_2 = 1/2$ ) whose EPR spectra in the absence of exchange consist of two  $\delta$ -like resonances.<sup>14</sup> As suggested by Abragam,<sup>18</sup> to obtain  $\varphi(t)$  in the cases when in the absence of exchange between dissimilar spins the spectra consist of two Lorentzian shaped resonances, it is necessary to

(19) Levstein, P. R.; Steren, C. A.; Gennaro, A. M.; Calvo, R. *Chem. Phys.* **1988**, *120*, 449.

(20) Sack, R. A. *Mol. Phys.* **1958**, *1*, 163.

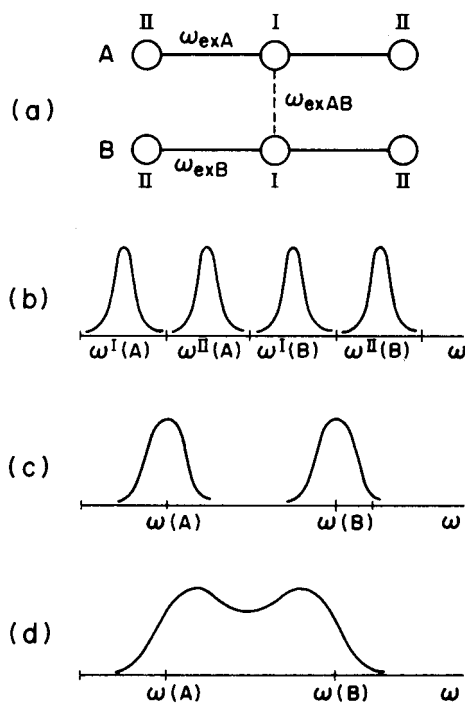


**Figure 3.** (a) Scheme of an extended system of copper ions with a structure consisting of four anisotropic spins ( $S = 1/2$ ) in two chains, called A and B. The spins  $S^I_\alpha$  and  $S^{II}_\alpha$  (with  $\alpha = A$  or B) are strongly coupled by the exchange interaction  $\omega_{\text{ex}\alpha}$ , while  $S^I_B$  and  $S^I_A$  (with  $i = I$  or II) are weakly coupled by  $\omega_{\text{exAB}}$ . EPR resonances considering  $\omega_{\text{exA}} = \omega_{\text{exB}} = \omega_{\text{exAB}} = 0$  (b), with  $\omega_{\text{ex}\alpha} > |\omega^I(\alpha) - \omega^{II}(\alpha)|$  and  $\omega_{\text{exAB}} = 0$  (c), and with  $\omega_{\text{ex}\alpha} > |\omega^I(\alpha) - \omega^{II}(\alpha)|$  and  $\omega_{\text{exAB}} < |\omega^I(B) - \omega^I(A)|$  (d).

add to the real diagonal matrix  $\omega$ , defined in eq 5, the complex diagonal matrix  $i\Gamma$  whose components are the half line widths of each resonance line. Then, including this correction in eq 7, it is possible to obtain for  $I(\omega)$

$I(\omega) \propto$

$$\frac{(\omega - \omega_c)^2(\Gamma_1 + \Gamma_2) + 2(\omega - \omega_c)\delta(\Gamma_1 - \Gamma_2) + [\delta^2 + \Gamma_1\Gamma_2 + \omega_{\text{ex}}(\Gamma_1 + \Gamma_2)](4\omega_{\text{ex}} + \Gamma_1 + \Gamma_2)}{[\delta^2 - (\omega - \omega_c)^2 + \Gamma_1\Gamma_2 + \omega_{\text{ex}}(\Gamma_1 + \Gamma_2)]^2 + [(2\omega_{\text{ex}} + \Gamma_1 + \Gamma_2)(\omega - \omega_c) + \delta(\Gamma_1 - \Gamma_2)]^2} \quad (7)$$

where

$$\omega_c = (\omega_1 + \omega_2)/2$$

$$\delta = (\omega_2 - \omega_1)/2$$

Anderson's result can be easily derived from eq 7 by making  $\omega_c = 0$  and  $\Gamma_1 = \Gamma_2 = 0$ . An expression for  $I(\omega)$  identical to eq 7 can be deduced from a model using modified Bloch equations. This method was originally introduced to analyze the effects of chemical exchange in NMR spectra, and it was used by Hoffmann et al.<sup>21</sup> to study the effect of exchange interactions in the EPR spectra of paramagnets.

Equation 7 may also be used to analyze the two-component EPR spectra arising from extended systems with four or more anisotropic spins coupled by exchange. Figure 3a shows a scheme of a crystal lattice corresponding to this case. In the absence of exchange interactions between dissimilar spins the EPR spectrum would consist of four resonance lines at the positions  $\omega^i(\alpha)$  (Figure 3b). However, if the pairs  $S^I_A - S^{II}_A$  and  $S^I_B - S^{II}_B$  are strongly coupled ( $\omega_{\text{ex}\alpha} > |\omega^I(\alpha) - \omega^{II}(\alpha)|$  or

equivalently  $J_\alpha > \mu_B B |g^I(\alpha) - g^{II}(\alpha)|$ ), the resonances corresponding to the spin pairs  $S^I_A - S^{II}_A$  and  $S^I_B - S^{II}_B$  would collapse each to a single line (Figure 3c). In addition, a weak exchange interaction  $\omega_{\text{exAB}}$  ( $\omega_{\text{exAB}} < |\omega^I(B) - \omega^I(A)|$  or equivalently  $J_{\text{AB}} < \mu_B B |g^I(B) - g^I(A)|$ ) coupling the spins  $S^I_A$  and  $S^I_B$  would produce a partial collapse of these two resonances (Figure 3d). In conclusion, this system may be modeled as two weakly exchange coupled spins  $S_A$  and  $S_B$ , which in the absence of the exchange interaction  $\omega_{\text{exAB}}$  have resonance frequencies  $\omega(A)$  and  $\omega(B)$ .

Fitting eq 7 to experimental spectra as in Figure 3d allows one to evaluate  $\omega_{\text{exAB}}$ , the positions  $\omega_1 = \omega(A)$  and  $\omega_2 = \omega(B)$ , and the widths  $\Gamma_1 = \Gamma_A$  and  $\Gamma_2 = \Gamma_B$  of the lines. These positions and widths do not take into account the shifts and broadening produced by the weak exchange  $\omega_{\text{exAB}}$ . Therefore,  $\Gamma_A$  and  $\Gamma_B$  are the self-widths of each resonance line originated by the interactions between all spins of the system, but time modulated by the exchange interaction between the strongly coupled spins. Thus, these values may be analyzed separately as corresponding to a strong exchange limit.

## Experimental Section

**Materials.** The compound Cu(asp)phen was prepared by mixing solid Cu(asp)(H<sub>2</sub>O)<sub>2</sub> suspended in hot water with a solution of the aromatic amine in methanol. The resulting blue solution was left to stand for several days, yielding deep blue irregular crystalline blocks. The crystal axes of the single-crystal samples were identified by measuring the angles between lateral faces with a goniometric microscope and by X-ray measurements.

**Magnetic Measurements.** Magnetic susceptibility ( $\chi$ ) measurements in powdered samples were performed using a SHE Corp. VTS 906 variable temperature magnetometer at a field of 1 kG, in the temperature range between 2 and 300 K. The data obtained were corrected for the diamagnetic contribution using Pascal constants.

EPR data in single crystals at 9.8 GHz were performed with a Bruker ER-200 EPR spectrometer, using a 12 in. rotating magnet and a Bruker cylindrical cavity with 100 kHz field modulation. A Varian E-line spectrometer and a cylindrical cavity were used for the 34.3 GHz measurements. All EPR experiments were carried out at room temperature. To orient the samples, a (001) face of the single crystals of Cu(asp)phen was glued to a cleaved KCl cubic holder, which defines a set  $x, y, z$  of orthogonal axes, with the  $x$  and  $y$  axes of the holder as the  $a$  and  $b$  axes of the sample, respectively. Then, the crystal direction  $c' = a \times b / |a \times b|$  was along the  $z$  axis of the sample holder. This holder was positioned in an horizontal plane at the top of a pedestal in the center of the microwave cavity, and the magnetic field  $\mathbf{B}$  was rotated in the  $xy$ ,  $zx$ , and  $zy$  planes of the samples.

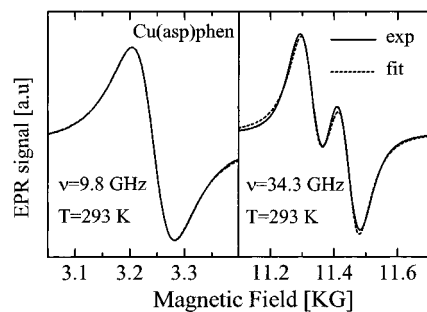
## Magnetic Susceptibility Data

A Curie-Weiss behavior  $\chi(T) = C_m / (T - \theta_c)$  was observed for Cu(asp)phen in the whole temperature range studied. A least squares fit of the data between 16 and 100 K gave  $C_m = 0.404$ -(2) emu-K/mol and an antiferromagnetic Curie temperature  $\theta_c = -0.49$ (1) K. These results are typical for a weakly exchange coupled compound.

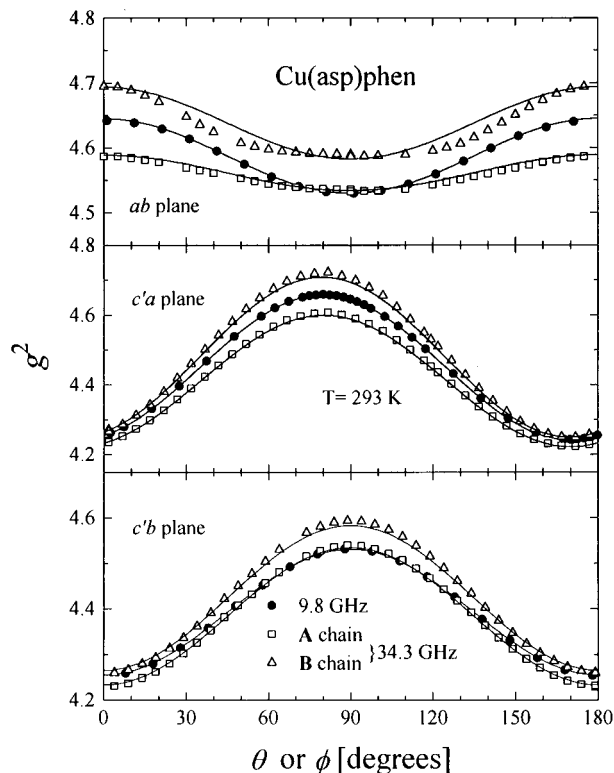
## EPR Data

Figure 4 shows the EPR spectra obtained in Cu(asp)phen with the magnetic field  $\mathbf{B}$  along the  $a$  crystal axis at 9.8 and 34.3 GHz, respectively. The spectra at 9.8 GHz were least squares fitted to the derivative of a single Lorentzian line, and those at 34.3 GHz to the derivative of eq 7. As we see above, fitting eq 7 to the experimental spectra allows one to compute positions and widths of the lines, and also  $\omega_{\text{ex}}$ . However, the values of  $\omega_{\text{ex}}$  obtained for field orientations where the EPR lines are close to the strong exchange limit are angular dependent. Only when the lines are well separated is  $\omega_{\text{ex}}$  constant as expected and

(21) Hoffman, S. K.; Waskowska, A.; Hilczler, W. *Solid State Commun.* **1990**, *74*, 1359.



**Figure 4.** EPR spectra obtained in Cu(asp)phen with the magnetic field  $\mathbf{B}$  along the  $a$  crystal axis at 9.8 and 34.3 GHz. The spectra at 9.8 GHz were least squares fitted to the derivative of a single Lorentzian line, and those at 34.3 GHz to the derivative of eq 7.



**Figure 5.** Angular variation of the crystal  $\mathbf{g}$ -tensors at 9.8 and 34.3 GHz for the magnetic field applied in the  $ab$ ,  $c'a$ , and  $c'b$  crystal planes of Cu(asp)phen. The data at 9.8 GHz correspond to the average of the molecular  $\mathbf{g}$ -tensors of the four magnetically nonequivalent copper ions of the unit cell. The data at 34.3 GHz correspond to each copper ion chain. The solid lines were obtained with the parameters given in Table 1 and the equation  $g^2(\theta, \phi) = \mathbf{h} \cdot \mathbf{g} \cdot \mathbf{g} \cdot \mathbf{h}$ , where  $\mathbf{h} = \mathbf{B}/|\mathbf{B}|$  is the magnetic field orientation.

predicted by eq 7. This is a weakness of eq 7 since good fits can be obtained with different parameters. Therefore, the value of  $\omega_{\text{ex}}$  obtained for field orientations far from the collapse of the lines was employed to fit all the spectra. Then, as shown in Figure 4, good agreement was obtained between the proposed functions and the experimental results at both microwave frequencies. Figures 5 and 6 display the angular variation of  $g^2(\theta, \phi)$  and the peak to peak line width  $\Delta B_{\text{pp}}(\theta, \phi)$  of the resonances, respectively, measured at 9.8 and 34.3 GHz.

**The  $\mathbf{g}$ -Factor.** In order to evaluate the components of the crystal  $\mathbf{g}$ -tensor defined in eq 2c, we performed a least squares fit of the function  $g^2(\theta, \phi) = \mathbf{h} \cdot \mathbf{g} \cdot \mathbf{g} \cdot \mathbf{h}$ , where  $\mathbf{h} = \mathbf{B}/|\mathbf{B}| = (\sin \theta \cos \phi, \sin \theta \sin \phi, \cos \theta)$  is the magnetic field orientation, to the data in Figure 5. The results obtained at both microwave frequencies given in Table 1 were employed to calculate the solid lines in Figure 5. According to eq 2c, the  $\mathbf{g}$ -tensor obtained

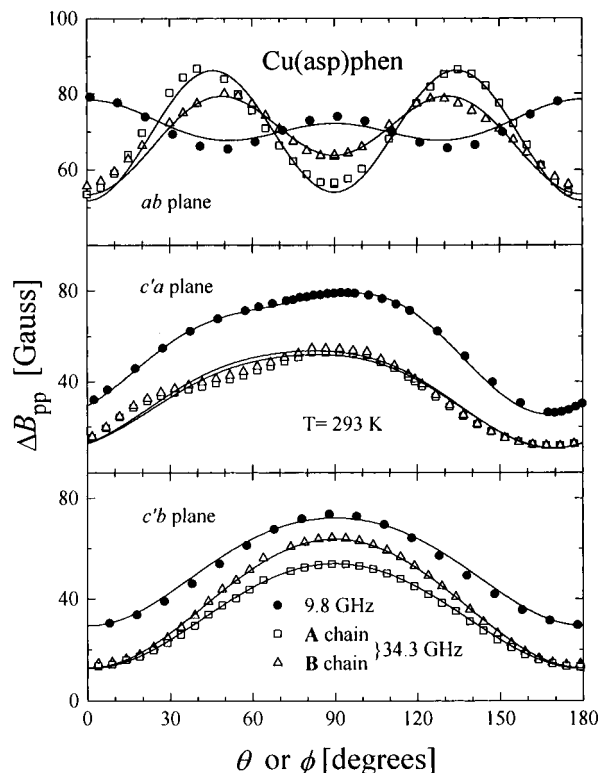


**Figure 6.** Angular variation of the peak-to-peak line width of the single exchange collapsed resonances at 9.8 GHz and for each component of the spectra at 34.3 GHz, for the magnetic field applied in the  $ab$ ,  $c'a$ , and  $c'b$  crystal planes of Cu(asp)phen. The data at 34.3 GHz correspond to each copper ion chain. The solid lines were obtained with the parameters given in Table 2 and eqs 9 and 10.

at 9.8 GHz is the average of the molecular  $\mathbf{g}$ -tensors of the four copper ions of the unit cell of Cu(asp)phen. The fact that a single resonance line is observed at 9.8 GHz indicates that the exchange interaction collapses the individual resonances of the magnetically nonequivalent copper ions, verifying

$$(i) \quad J_A > |g^I(A) - g^{II}(A)|\mu_B B$$

$$(ii) \quad J_B > |g^I(B) - g^{II}(B)|\mu_B B$$

$$(iii) \quad J_{AB} > |g^i(A) - g^j(B)|\mu_B B \quad (\text{with } i = \text{I or II}) \quad (8)$$

where  $J_A$  is the exchange parameter associated with the  $\sigma$ -skeleton of the asp molecule,  $J_B$  is that associated with the chemical path including a carboxylate bridge plus a hydrogen bond, and  $J_{AB}$  is that associated with the chemical paths connecting both copper ion chains (Figures 1 and 2). Since at 34.3 GHz the EPR spectra display two components, the above three conditions are not verified simultaneously. Obviously each component of the spectra at 34.3 GHz arises from the collapse due to the exchange interaction between two magnetically nonequivalent copper ions. For symmetry reasons, in the  $abc'$  crystal axis system the components of the molecular tensors associated with copper ions related by a  $C_{2b}$  symmetry operation differ only in the sign of the  $xy$  and  $zy$  components.<sup>22</sup> Then, the symmetry-related copper ions [Cu<sup>I</sup>( $\alpha$ ) and Cu<sup>II</sup>( $\alpha$ ), with  $\alpha = \text{A or B}$ ] are magnetically equivalent in the  $c'a$  plane and their EPR spectra are equal. The observation of spectra having two components in this plane indicates that condition iii is not

(22) Calvo, R.; Oseroff, S. B.; Abache, H. C. *J. Chem. Phys.* **1980**, *72*, 760.

**Table 1.** Components of the crystal  $g^2$  Tensors obtained by a Least Squares Fit of the Data in Figure 5 Obtained at Both Microwave Frequencies<sup>a</sup>

	9.8 GHz	34.3 GHz	
		Cu(A)	Cu(B)
$(g^2)_{xx}$	4.6451(3)	4.589(1)	4.694(1)
$(g^2)_{yy}$	4.5304(3)	4.534(1)	4.583(1)
$(g^2)_{zz}$	4.2553(3)	4.233(1)	4.265(1)
$(g^2)_{zx}$	0.0721(3)	0.064(1)	0.081(1)
$(g^2)_{xy} = (g^2)_{zy}$	0.0000(3)	0.000(1)	0.000(1)
$(g^2)_1$	4.2424(3)	4.222(1)	4.250(1)
$(g^2)_2$	4.6580(3)	4.600(1)	4.709(1)
$(g^2)_3$	4.5304(3)	4.534(1)	4.583(1)
$\mathbf{a}_1$	-0.1761(7), 0, 0.9844(1)	-0.184(2), 0, 0.9829(4)	-0.170(2), 0, 0.9854(3)
$\mathbf{a}_2$	0.9844(1), 0, 0.1761(7)	0.9829(4), 0, 0.184(2)	0.9854(3), 0, 0.170(2)
$\mathbf{a}_3$	0,1,0	0,1,0	0,1,0
$g_{  }$		2.216(1)	2.241(1)
$g_{\perp}$		2.055(1)	2.064(1)
$\theta_m, \theta_c$		82.7, 82.8	82.1, 81.8
$\phi_m, \phi_c$		42.7, 44.5	40.9, 39.8
$2\alpha_m, 2\alpha_c$		95.5, 91.9	99.2, 101.5

<sup>a</sup>  $(g^2)_1$ ,  $(g^2)_2$ , and  $(g^2)_3$  and  $\mathbf{a}_1$ ,  $\mathbf{a}_2$ , and  $\mathbf{a}_3$  are the eigenvalues and eigenvectors, respectively. The values of  $g_{||}$  and  $g_{\perp}$ , the polar and azimuthal angles ( $\theta_m$ ,  $\phi_m$ ) of the normals to the square of ligands to copper ions, and the angle between these normals to copper ions in sites I and II ( $2\alpha_m$ ) obtained from the EPR data at 34.3 GHz and the corresponding crystallographic values ( $\theta_c$ ,  $\phi_c$ ,  $2\alpha_c$ ) are also included.

satisfied at 34.3 GHz. However, we cannot make conclusions about conditions i and ii. As shown in Table 1, the crystal  $g$ -tensors obtained at 34.3 GHz have zero  $xy$  and  $zy$  components, a result expected for a system with two magnetically nonequivalent copper ions related by a  $C_{2b}$  symmetry operation, whose EPR spectra display a single exchange collapsed resonance line.<sup>23</sup> This fact allows us to verify that each component of the spectra is the result of the collapse by exchange of the resonances belonging to the symmetry-related copper ions. Therefore conditions i and ii still hold at 34.3 GHz, and the exchange frequency  $\omega_{ex}$  associated with the exchange parameter  $J_{AB}$  is obtained from the fit of the spectra with eq 7 and allows us to obtain  $|J_{AB}/k| = 2.7(6)$  mK for the exchange interaction between different types of copper ion chains (Figures 1 and 2).

In order to calculate the molecular  $g$ -factors of each type of copper ion we used the method described in ref 23 assuming axially symmetric molecular  $g$ -tensors. We defined  $\theta_m$  and  $\phi_m$  as the polar and azimuthal angles corresponding to the direction along which  $g_{||}$  is measured. Then, we calculated  $g_{||}$ ,  $g_{\perp}$ ,  $\theta_m$ , and  $\phi_m$  using the values of the four nonzero components given in Table 1, which shows that the results of these calculations are in good agreement with the corresponding crystallographic values. This procedure also allowed us to identify the crystal  $g$ -tensor corresponding to each type of copper ion chain.

The components obtained considering axial symmetry for the molecular  $g$ -tensors would indicate  $d(x^2-y^2)$  ground state orbitals for the Cu(A) and Cu(B) ions.<sup>24</sup> However, the differences of the molecular  $g$ -factors of the copper ions (Table 1) cannot be explained considering a model with axial symmetry, since in this case the  $g$ -values are independent of the distance Cu-O<sub>ap</sub>.<sup>24</sup> Hitchman et al.<sup>25</sup> studied a series of compounds with copper sites similar to Cu(asp)phen. They found that the trace of the molecular  $g$ -tensors increases progressively in conjunction with the strength of the axial ligand field. These results agree with those obtained in Cu(asp)phen, suggesting also that the ground state orbital for the Cu(A) and Cu(B) ions is given mainly by the  $d(x^2-y^2)$  orbital, having a small admixture of the  $d(z^2)$ .

**Table 2.** Values of the Parameters (in gauss) Obtained by Fitting the Peak to Peak Line Width Data Shown in Figure 6 with Eq 9<sup>a</sup>

	9.8 GHz	34.3 GHz	
		Cu(A)	Cu(B)
$a_1$	64.4(7)	47(1)	48(1)
$a_2$	58.3(7)	49(1)	58(1)
$a_3$	16.2(8)	8(1)	8(1)
$a_4$	4.2(4)	5.7(5)	6.5(5)
$a_5$	$16(1) \times 10^{-4}$	$6(1) \times 10^{-4}$	$6(1) \times 10^{-4}$
$b$		$57(1.5) \times 10^2$	$30(1.1) \times 10^2$

<sup>a</sup> In the case of the data at 34.3 GHz we include the coefficient  $b$  considering the contribution of the residual Zeeman interaction given in eq 10.

**Line Width Data.** The angular variation of the EPR line width of the single exchange collapsed resonance obtained at 9.8 GHz (Figure 6) is well accounted for with an angular function which includes the second moment of the dipolar interaction,<sup>26</sup> plus four terms having angular dependencies according to the crystal symmetry

$$\Delta B_{pp}(\theta, \phi) = a_1 \sin^2 \theta \cos^2 \phi + a_2 \sin^2 \theta \sin^2 \phi + a_3 \cos^2 \theta + a_4 \sin \theta \cos \theta \cos \phi + a_5 M_2^{\text{dip}} \quad (9)$$

where  $\theta$  and  $\phi$  are referred to the crystal axis system  $abc'$ . The values of the coefficients  $a_i$  are given in Table 2 and were employed to obtain the solid lines in Figure 6. The magnitudes of these coefficients are a consequence of perturbations contributing to the Hamiltonian of eq 3 such as hyperfine, dipolar, and antisymmetric and anisotropic exchange. They are not important for our purposes and will not be analyzed in detail.

The line width data obtained at 34.3 GHz shows a different behavior for each type of copper ion chain. In the  $c'a$  and  $c'b$  planes they follow an angular variation similar to that observed at 9.8 GHz, indicating that the broadening mechanism is similar at both microwave frequencies. The line widths in the  $ab$  plane are frequency-dependent, indicating a broadening arising from the contribution of the residual Zeeman interaction.<sup>9,19</sup> In the case of two magnetically nonequivalent copper ions this contribution is given by<sup>19</sup>

(23) Calvo, R.; Mesa, M. A. *Phys. Rev. B* **1983**, *28*, 1244.

(24) Zeiger, H. J.; Pratt, G. W. *Magnetic Interactions in Solids*; Oxford University Press: London, 1973.

(25) Hitchman, M.; Kwan, L. *J. Chem. Soc., Dalton Trans.* **1987**, 457.

(26) Slichter, C. P. *Principles of Magnetic Resonance*; Springer: Berlin, 1990.

$$\Delta B_{pp}^{Fz}(\theta, \phi) = \frac{\sqrt{\frac{2}{3}}\pi[g^1(\theta, \phi) - g^{II}(\theta, \phi)]^2 \omega_0^2 \hbar}{4g^3(\theta, \phi)\mu_B \omega_{ex\alpha}} \quad (10)$$

where the  $\omega_{ex\alpha}$  are the exchange frequencies, related to their corresponding exchange parameters by<sup>19</sup>

$$\omega_{exA}^2 = 2J_A^2/\hbar^2 \quad (11a)$$

$$\omega_{exB}^2 = 2J_B^2/\hbar^2 \quad (11b)$$

Equation 10 contributes to the line width only in the *ab* and *c'b* planes where the copper ions are magnetically nonequivalent. The frequency independent behavior obtained in the *c'b* plane is due to the small difference between the molecular *g*-factors of the symmetry-related copper ions occurring in this plane.

In order to evaluate the angular variation of the line width at Q-band, the data in Figure 6 were least squares fitted with eqs 9 and 10. In Table 2 we include the values of the *a<sub>i</sub>* coefficients of eq 9 and the *b* coefficient associated with eq 10, and these values are employed to obtain the solid lines in Figure 6. From the *b* coefficients we calculated the exchange frequencies  $\omega_{exA} = 1.4 \times 10^{11} \text{ s}^{-1}$  and  $\omega_{exB} = 2.7 \times 10^{11} \text{ s}^{-1}$ , and using eqs 11 we obtained the exchange parameters  $|J_A/k| = 0.77(2) \text{ K}$  and  $|J_B/k| = 1.44(2) \text{ K}$  between neighboring copper spins in the A and B chains, respectively.

### Exchange Interactions and Superexchange Paths

In Cu(asp)phen we have three different chemical paths which are able to transmit superexchange interactions (Figures 1 and 2). The exchange parameter  $|J_A/k| = 0.77(2) \text{ K}$  is attributed to the interaction transmitted through the asp molecule (Figure 2). This value is 1 order of magnitude smaller than that obtained for the  $\sigma$  skeleton of the asp molecule in Cu(asp) ( $J/k = -5.3 \text{ K}$ ).<sup>8</sup> The structural characteristics of the asp molecule in both compounds are similar, differing only in the side chain carboxylic oxygen, which is bonded to a copper ion in an equatorial position in Cu(asp), and through an apical position in Cu(asp)phen. The smaller sharing of the carboxylic oxygen electron density with the ground state orbital of the copper ions in Cu(asp)phen is the main factor that could produce the observed decrease of the exchange coupling.

The exchange parameter  $|J_B/k| = 1.44(2) \text{ K}$  is associated with the double chemical path formed by a carboxylate bridge plus a hydrogen bond (Figure 2). The ability of a similar chemical path to transmit the exchange interaction was previously evaluated in Cu(asp)bpy ( $|J/k| = 0.20 \text{ K}$ ).<sup>12</sup> The fact that one of the double chemical paths in Cu(asp)phen has both copper ligands in apical positions could explain the obtained greater value.

The weak exchange interaction  $|J_{AB}/k| = 2.7(6) \text{ mK}$  between dissimilar copper ions arises from a complex network of hydrogen bonds and hydrophobic interactions between the aromatic amines, shown in Figures 1 and 2. One of these chemical paths involves three consecutive hydrogen bonds connecting one copper ion ligand in an apical position and other in an equatorial position. These characteristics and the long metal-metal distance predict a negligible superexchange interaction through this chemical path.<sup>27</sup> The ability of a hydrophobic interaction as superexchange path was suggested in refs 11 and 12. The results obtained in Cu(asp)phen also suggest that the hydrophobic interactions contribute with a weak but not negligible exchange interaction. However, this result cannot be compared with the *J* values obtained in other compounds due to the different methods employed in their determination.

### Conclusions

We report EPR and magnetic susceptibility measurements in an exchange coupled extended system with two dissimilar copper ions. The EPR results are analyzed in terms of Anderson's model for a system in the weak exchange limit and the exchange narrowing model in the strong exchange limit. The results obtained with these models allow us to evaluate selectively the electronic properties of the dissimilar copper ions and the exchange parameters associated with the chemical paths connecting them in the crystal lattice. The electronic properties are those expected for the copper ions in square pyramidal coordination, and the differences encountered are associated with the different lengths of the Cu-O<sub>ap</sub> bond. We have also evaluated the ability of chemical paths including saturated hydrocarbonated chains, hydrogen bonds, and hydrophobic interactions to transmit the exchange interaction. The role of hydrophobic interactions in a superexchange path is still unclear. The distance of about 3.5 Å between the interacting aromatic amines discards a possible  $\sigma$  bond, and in principle, the associated *J* values would be negligible. Further experimental and theoretical work should be carried out in order to clarify this point. With this purpose, we are looking for compounds with copper ions connected only by hydrophobic interaction in order to evaluate the associated *J* values that can be related to their structural characteristics.

**Acknowledgment.** This work was supported by Universidad Nacional del Litoral (CAI+D 291 93/94) and CONICET (PID 3761/92) in Argentina, Universidad de Chile (DTI Project Q3567-9633) and Fundación Andes in Chile, and cooperation programs CNRS(France)-CONICYT (Chile) and Fundación Vitae (Brazil-Argentina).

IC9610501

(27) Hoffmann, S. K.; Hilczler, W.; Goslar, J. *Appl. Magn. Reson.* **1994**, *7*, 289.